



# Combined Magnetostratigraphy From Three Localities of the Rainstorm Member of the Johnnie Formation in California and Nevada, United States Calibrated by Cyclostratigraphy: A 13R/Ma Reversal Frequency for the Ediacaran

Kenneth P. Kodama\*

#### **OPEN ACCESS**

Department of Earth and Environmental Sciences, Lehigh University, Bethlehem, PA, United States

#### Edited by:

John William Geissman, The University of Texas at Dallas, United States

# Reviewed by:

Mark Hounslow, Lancaster University, United Kingdom Daniel J. Peppe, Baylor University, United States Cor Langereis, Utrecht University, Netherlands

## \*Correspondence:

Kenneth P. Kodama kpk0@lehigh.edu

#### Specialty section:

This article was submitted to Geomagnetism and Paleomagnetism, a section of the journal Frontiers in Earth Science

> Received: 25 August 2021 Accepted: 28 October 2021 Published: 24 November 2021

#### Citation:

Kodama KP (2021) Combined Magnetostratigraphy From Three Localities of the Rainstorm Member of the Johnnie Formation in California and Nevada, United States Calibrated by Cyclostratigraphy: A 13 R/Ma Reversal Frequency for the Ediacaran. Front. Earth Sci. 9:764714. doi: 10.3389/feart.2021.764714 A combined magnetostratigraphy for the Rainstorm Member of the Ediacaran Johnnie Formation was constructed using the sediment accumulation rates determined by rock magnetic cyclostratigraphy for three localities of the Rainstorm Member to provide a high resolution, time-calibrated record of geomagnetic field reversal frequency at a critical time period in Earth history. Two previously reported magnetostratigraphy records from Death Valley, California, the Nopah Range and Winters Pass Hills (Minguez et al., 2015), were combined with new paleomagnetic and cyclostratigraphic results from the Desert Range locality of the Rainstorm Member in south central Nevada, United States . The Johnnie oolite marker bed is at the base of each of the three sections and allows their regional correlation. The Nopah Range and Desert Range localities have similar sediment accumulation rates of ~5 cm/ka, so their stratigraphic sections can be combined directly. The Winters Pass Hills locality has a higher sediment accumulation rate of 8.4 cm/ka, therefore its stratigraphic positions are multiplied by 0.6 to combine with the Desert Range and Nopah Range magnetostratigraphy. The thermal demagnetization results from the Desert Range locality isolates characteristic remanent magnetizations that indicate two nearly antipodal east-west and shallow directions and a mean paleopole (11.7°N, 348.4°E) that is consistent with "shallow" Ediacaran directions. The Desert Range also yields a magnetic susceptibility rock magnetic cyclostratigraphy that records short eccentricity, obliquity, and precession astronomically-forced climate cycles in the Ediacaran. The high-resolution combined magnetostratigraphy with nearly meter-scale stratigraphic spacing (nominally 23 ka, based on the Desert Range sediment accumulation rate), indicates 11 polarity intervals in a cyclostratigraphy-calibrated duration of 849 ka, indicating a reversal frequency of 13 R/Ma. The Rainstorm Member records the Shuram carbon isotope excursion, hence its age is ~574 Ma. Given the recent cyclostratigraphycalibrated reversal frequency of 20 R/Ma from the Zigan Formation (Levashova et al., 2021)

1

at 547 Ma, our results show that reversal frequency was high but fluctuated during the Ediacaran.

Keywords: magnetostratigraphy, cyclostratigraphy, johnnie formation, ediacaran, reversal frequency

#### INTRODUCTION

Evidence has been accumulating that the reversal rate of the Earth's magnetic field was extremely high in the latest Precambrian/earliest Paleozoic. Magnetostratigraphy studies from Ediacaran rocks (e.g., Pavlov and Gallet, 2010; Bazhenov et al., 2016; Meert et al., 2016) or middle Cambrian rocks (Pavlov and Gallet, 2001; Gallet et al., 2019) show large numbers of polarity reversals in sedimentary stratigraphic sections. Although all these studies showed a high reversal frequency based on estimated sediment accumulation rates, only the most recent study of the Ediacaran Zigan Formation from the Urals (Levashova et al., 2021) presented a calibrated sediment accumulation rate using rock magnetic cyclostratigraphy (Kodama and Hinnov, 2014). The Zigan Formation is dated to be 547 Ma in the latest Ediacaran, just before the Cambrian explosion of life at about 540 Ma. The reversal frequency obtained from Levashova et al. (2021) is 20 R/Ma (reversals per million years). For comparison, the highest reversal frequency, over the past 170 Ma, based on the sea floor magnetic anomaly record of geomagnetic polarity, is 10-12 R/Ma for the latest Jurassic/early Cretaceous. The polarity stratigraphy record from the astronomically-calibrated Newark Basin rocks (Kent et al., 2017), provides a well-calibrated record of reversals earlier than the Jurassic/Cretaceous during the Triassic and indicates 66 polarity intervals in the 33.2 million year period from 199.5 Ma to 232.7 Ma or an average reversal frequency of about 2 R/Ma. Hüsing et al. (2014) provide an astronomically-calibrated magnetostratigraphy in Lower Jurassic marine sediments from the United Kingdom and also indicate a low (~2-3 R/Ma) reversal frequency at about 200 Ma. Li et al. (2017) see polarity reversal patterns in the astronomically-calibrated magnetostratigraphy Triassic Xujiahe Formation of South China similar to those in the coeval Newark supergroup rocks.

# Rainstorm Member of the Johnnie Formation

Our study has recovered a high reversal frequency from the Rainstorm Member of the Ediacaran Johnnie Formation. The Rainstorm Member is the most widespread member of the Johnnie Formation outcropping throughout the southern Death Valley-Kingston Range area in California, the Spring Mountains, the Nevada Test Site and in the Desert Range of Nevada. It contains three units, the siltstone unit, the carbonate unit and the siltstone and quartzite unit. The basal siltstone unit is thin, typically less than 30 m thick. The overlying carbonate unit is comprised of pale-red to grey-red siltstone and limey silt. It ranges from 50–80 m in thickness (Stewart, 1970) and is the main unit sampled in this study. The base of our sampled section is

marked by the Johnnie Oolite, a 2–3 m thick oolitic dolomite which occurs near the middle or in the upper half of the siltstone unit (Stewart, 1970). It serves as a marker bed to which the base of the stratigraphic sections at different localities are tied. This is important because it allows the stratigraphic positions of paleomagnetic data collected at various localities of the Rainstorm Member to be very accurately combined, critical for the magnetostratigraphy that we will present in this paper. The top portions of the sections are correlated by extending the sediment accumulation rates derived from the magnetic susceptibility cyclostratigraphy. In the section sampled in this study the Rainstorm Member strikes 326° and dips 45° to the northeast. Structural deformation in the area is related to displacements along Mesozoic and Tertiary thrust systems and strike-slip faults (Stewart, 1970).

We initially studied the Rainstorm Member of the Johnnie Formation because it carries a record of the Shuram carbon isotope excursion (LeGuerroue et al., 2006). The Shuram is the largest negative carbon isotope excursion in Earth history with a nadir of approximately  $-12 \delta^{13}$ C in inorganic carbon occurring globally just before the Cambrian explosion of multi-cellular life (Knoll and Carroll, 1999). Minguez et al. (2015) used magnetic susceptibility cyclostratigraphy and magnetostratigraphy to determine the duration of the Shuram excursion in the Johnnie Formation rocks. Minguez et al.'s (2015) rock magnetic, magnetic susceptibility, cyclostratigraphic study of the Rainstorm Member at the Nopah Range and Winters Pass Hills observed spectral peaks that were identified as short eccentricity, obliquity and precession Milankovitch cycles. We also studied the duration of the Shuram in the Wonoka Formation in Australia (Minguez and Kodama, 2017) and the Doushantuo Formation in south China (Gong et al., 2017). In all three studies we found a duration of 8-9 Ma for the Shuram carbon isotope excursion using rock magnetic, either magnetic susceptibility or anhysteretic remanent magnetization (ARM), cyclostratigraphy. We also found a normal polarity interval at the nadir of the carbon isotope excursion in Death Valley, California and in South Australia providing evidence that the excursion was synchronous globally (Minguez and Kodama, Investigating this relationship between field polarity and the nadir of the excursion was not possible in China because the Doushantuo Formation was found to be remagnetized in the Mesozoic (Gong et al., 2017; Gong et al., 2019).

We studied the Rainstorm Member of the Johnnie Formation at two localities in the Death Valley region, the Nopah Range and Winters Pass Hills (Minguez et al., 2015). (Van Alstine and Gillette 1979) reported a magnetostratigraphic study of the Rainstorm Member from the Desert Range of south-central Nevada about 130 km northeast of the Nopah Range and Winters Pass Hills localities. Our initial intent was to conduct a magnetostratigraphy and rock magnetic cyclostratigraphy study



FIGURE 1 | Google Earth image of the sampling area in the Desert Range, Nevada. Black lines show contacts of late Precambrian and early Cambrian formations in the area based on a map in (Van Alstine and Gillet 1979) with formation age getting younger from left to right. The two locations sampled are shown.

of the Rainstorm Member in the Desert Range to investigate the relationship of a normal polarity event with nadir of the Shuram carbon isotope excursion.

One critical aspect of our study is the age of the reversal frequency we observed in the Rainstorm Member. The Rainstorm Member records the onset of the Shuram carbon isotope excursion including its nadir. The end of the Shuram excursion has been dated at 550.55 ± 0.75 Ma (Condon et al., 2005) from an ash bed that was initially interpreted to be at the very top of the Doushantuo Formation. However, (An et al., 2015), work on the upper part of the Doushantuo Fm in the Three Gorges area suggests that the euxinic shale that records the end of the Shuram excursion (Member 4 of the Doushantuo Formation). is not directly below the ash layer dated by Condon et al. (2005), and hence the end of the Shuram may be much older than previously thought. Rooney et al. (2020) report Re-Os ages from different continents of the onset (574  $\pm$  4.7 Ma) and end (567  $\pm$ 3.0 Ma) of the Shuram carbon isotope excursion. This would suggest the Rainstorm rocks we studied are approximately 574 Ma in age.

In this paper, we combine magnetostratigraphy results from the Rainstorm Member of the Johnnie Formation collected at three localities: the Nopah Range and Winters Pass Hills in Death Valley and the Desert Range in Nevada. The magnetostratigraphies are accurately combined using magnetic susceptibility cyclostratigraphy (Kodama and Hinnov, 2014) and the resulting reversal frequency is time calibrated using the rock magnetic cyclostratigraphy.

## **METHODS**

We received permission from Nellis Air Force Base and from the Desert National Wildlife Refuge to sample the Rainstorm Member for 2 days in May 2018. Both entities control the sampling locality. The target area was that initially sampled by Van Alstine and Gillett (1979). **Figure 1** shows the two locations in this area where we were able to locate exposures of the

Rainstorm Member. Location 1 (Sites JO-7; **Figure 1**) gave us access to the bottom 7 m of the Rainstorm Member, including the Johnnie Oolite. Oriented hand samples were collected every meter of section. 25 mm diameter cores were drilled from these hand samples for paleomagnetic measurement and demagnetization at Lehigh University. At least three cores were drilled from each hand sample. Location 2 (Sites 16.5–45; **Figure 1**) allowed us to sample from 16.5 to 45 m above the Johnnie Oolite, which was also exposed at this location and thus allowed an accurate stratigraphic position for our sites. We sampled this location with a gasoline-powered modified chain saw drill (Pomeroy). We drilled three independently oriented samples per horizon and sampled the section at nominally 2 m stratigraphic intervals.

Unoriented rock samples approximately  $3 \times 3 \times 3$  cm in size were collected every 25 cm of section for the rock magnetic cyclostratigraphy study at both locations 1 and 2. The section was sampled nearly continuously for 45 m, with the exception of the stratigraphic gap between 7 and 16.5 m, where no exposures could be located in the 2 days of access we were granted.

The oriented paleomagnetic core samples were stepwise thermally demagnetized in a single chamber ASC Model TD-48SC thermal demagnetizer in 10-20 steps between 100-200°C and 680°C. Remanence was measured in a 2G Enterprises 755 superconducting rock magnetometer. thermal Both demagnetization and remanence measurement were conducted in a magnetostatically-shielded room built by Lodestar Magnetics (ambient field intensity ~350 nT) in the Paleomagnetism Laboratory of Lehigh University. The bulk susceptibility of the unoriented cyclostratigraphy samples was measured using an Agico KLY-3s Kappabridge at Lehigh University. Three measurements were made on each sample and averaged. The susceptibility measurements were normalized by mass. The Kappabridge was also used to measure the temperature dependence of susceptibility from liquid nitrogen temperature (-196°C) to 0° and from 20°C to 700°C in order to identify magnetic mineralogy and the relative proportion of ferromagnetic and paramagnetic mineral contributions to the bulk susceptibility.

Principal component analysis was carried out on vector endpoint diagrams (Kirschvink, 1980) using the PmagPy software (Tauxe et al., 2016). Spectral analysis of the magnetic susceptibility time series was conducted using the  $2\pi$  multi-taper method (MTM, Thomson, 1982). Before spectral analysis the time series was resampled at a 0.36 m even spacing using linear interpolation and a Lowess detrending model with a 35% window was applied. Spectral peak significance was estimated by robust red noise and its confidence limits at 90, 95, 99% calculated from Mann and Lees (1996). These calculations were carried out using the Acycle (v 2.0) software (Li et al., 2019).

Carbon isotope ( $\delta^{13}$ C) values were measured for 24 samples from the Rainstorm member in order to determine if the rocks had recorded the Shuram carbon isotope excursion. Initially the objective was to determine the stratigraphic position of the nadir of the excursion for comparison to the magnetostratigraphy, but

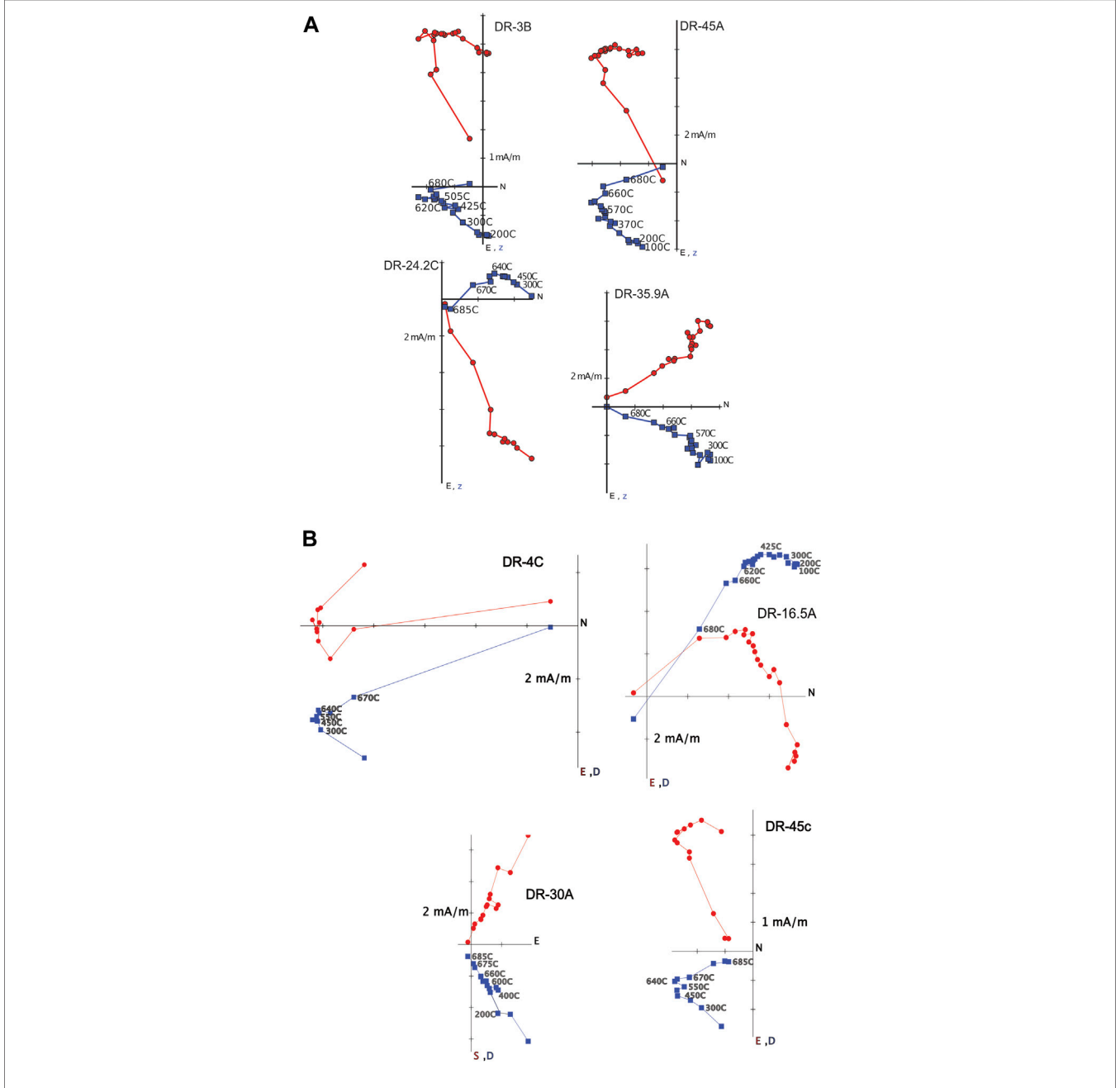
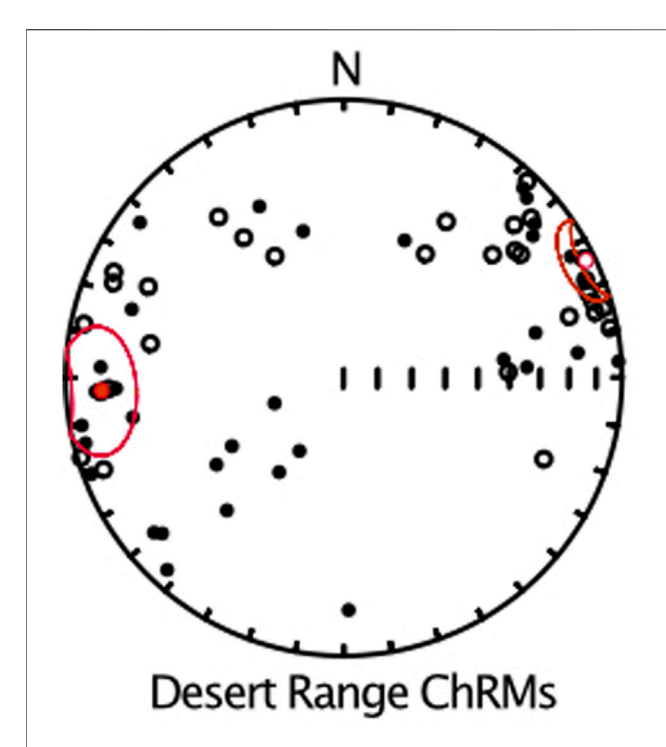


FIGURE 2 | (A) Vector endpoint diagrams for the stepwise thermal demagnetization of the Rainstorm Member samples. Red circles are horizontal component, blue squares are vertical component. Stratigraphic coordinates. Samples DR-3B, DR-45A, and DR-35.9A show the westerly ChRM, Sample DR-24.2C shows the more easterly ChRM. (B) Vector endpoint diagrams for the stepwise thermal demagnetization of Rainstorm Member samples with intermediate directions and VGPs. Same symbols as in (A). Note the clear separation of low temperature and high temperature components except for sample 30A.

ultimately the goal was to compare the carbon isotope values with those observed in the Rainstorm Member at the Nopah Range and Winters Pass Hills localities in Death Valley (Minguez et al., 2015). The Desert Range samples spanned the complete 45 m section at a 2 m stratigraphic interval, with the exception of the 9.5 m gap between 7 m and 16.5 m. The  $\delta^{13}$ C values were measured on carbonate by a Thermo Gas Bench II connected

to a Delta Advantage mass spectrometer in continuous flow mode at the Department of Geology, Union College. Reference standards (LSVEC, NBS-18, and NBS-19) were used for isotopic corrections and to assign the data to the appropriate isotopic scale using linear regression. The analytical uncertainty is  $\pm 0.02\%$  (VPDB) based on 7 NBS-19 standards over two analytical sessions.



**FIGURE 3** | Characteristic remanence directions for the thermal demagnetization data of the Rainstorm Member from the Desert Range. Open circles, upper hemisphere, filled in circles, lower hemisphere. Red lines show mean directions for the western set of directions (normal polarity) and eastern set of directions (reversed polarity) along with their  $\alpha_{95}$  circles of 95% confidence. Intermediate directions cluster in the southwest and toward the north.

# **RESULTS**

## **Paleomagnetic Analysis**

Principal component analysis of the thermal demagnetization vector endpoint diagrams (Zijderveld, 1967) isolated a characteristic remanent magnetization (ChRM) typically between the temperatures of 580°C and 680°C (Figure 2). Maximum angular deviations (MADs) of the fit ranged from 1.3° to, in one case, as high as 17.4°, but averaged 6.1° for 60 samples from 22 horizons. An equal area net plot of the ChRMs (Figure 3) clearly shows two nearly antipodal groups of directions indicating that in most cases a polarity assignment could be made. One direction is nearly due west and flat  $(D = 268.7^{\circ}, I = 11.7^{\circ}, N = 31, \alpha_{95} = 17.0^{\circ})$  which is interpreted to be normal polarity, based on North America's paleogeography in the late Precambrian (Cocks and Torsvik, 2011). The other direction is  $155.6^{\circ}$  away pointing northeast and flat (D =  $65.0^{\circ}$ , I =  $-4.8^{\circ}$ , N = 29,  $\alpha_{95} = 9.6^{\circ}$ ). Even given the uncertainties, the directions do not pass a reversals test, but polarity assignments can be made based on the great circle distance between the virtual geomagnetic poles (VGPs) calculated for these directions and the mean VGP (paleomagnetic pole) determined from these data. In addition to the two nearly antipodal groups of ChRMs, there are other groupings of directions (Figure 3). There are ChRM directions to the southwest and down with intermediate inclinations and also ChRM directions to the north with either intermediate up or down inclinations (Figure 3).

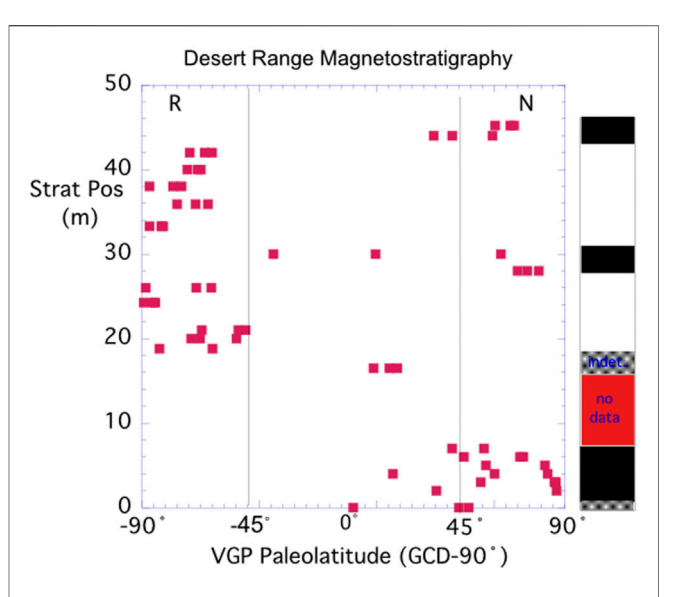


**FIGURE 4** | Magnetostratigraphy for the Rainstorm Member samples from the Desert Range. The VGP paleolatitude (great circle distance of each sample's VGP from the mean paleomagnetic pole –90°) for the Rainstorm Member is plotted as a function of stratigraphic position. Note the 9.5 m gap in data between 7 m and 16.5 m which will be filled in the combined magnetostratigraphy developed using the Nopah Range and Winters Pass Hills data.

The Desert Range magnetostratigraphy (**Figure 4**) shows the intermediate VGP latitudes that result from these directions at about 1–4 m, 16.5, 30, and 45 m in the section. Vector endpoint diagrams (**Figure 2B**) for samples from these horizons show a clear separation between a low temperature magnetization component (<500°C-600°C) and the high temperature ChRM component, with the exception of the sample at 30 m. At the 30 m horizon two samples have intermediate directions (north and down), but one sample is clearly normal polarity. In this case the intermediate ChRM directions could be due to a poorly resolved high temperature component or one that is contaminated by the low temperature component. At horizons 16.5 and 45 m the intermediate ChRM directions occur near polarity interval boundaries and could be recording true transitional directions.

In about 60% of the samples, the low temperature magnetization component is observed and is clearly separate from the high temperature ChRM. The low temperature component is typically isolated between 200°C and  $500^{\circ}$ – $600^{\circ}$ C (**Figures 2A,B**) and has a stratigraphic mean direction (D = 9°, I = 43°) similar to a low temperature component observed by Minguez et al. (2015) in the Rainstorm member of the Johnnie Formation in the Nopah Range, Death Valley, California. Minguez et al. (2015) attributed the low temperature Nopah Range component to Miocene age overprinting, based on its similarity to the North American Miocene paleopole (Torsvik et al., 2012). We suggest the same origin for the Desert Range low temperature component.

The paleomagnetic pole for the Rainstorm Member of the Johnnie Formation collected at the Desert Range is 11.7°N,

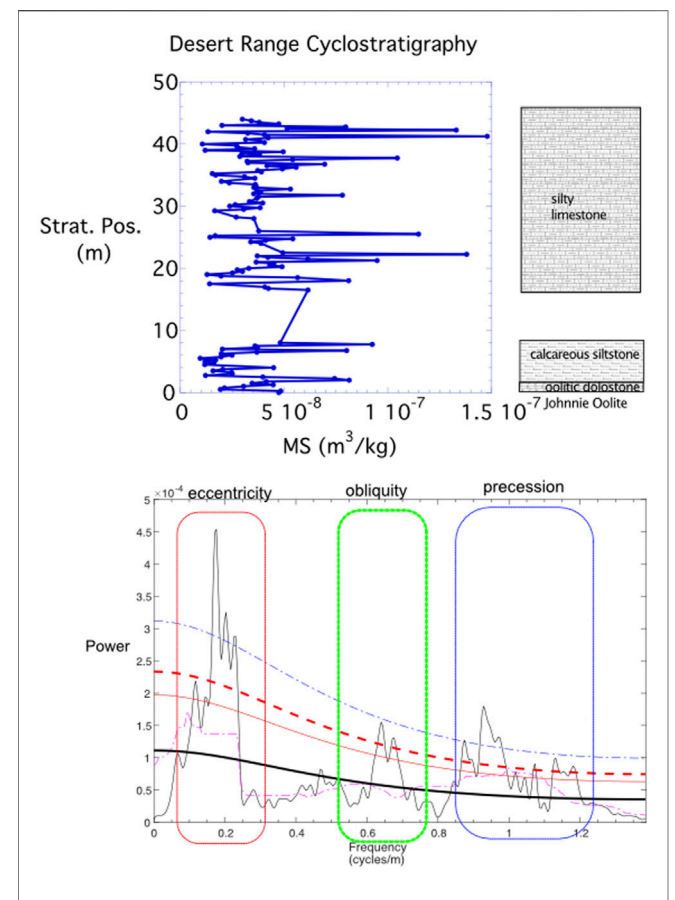


**FIGURE 5** | Desert Range Cyclostratigraphy. **(top)** Mass normalized magnetic susceptibility  $\langle \chi \rangle$  data series for the Desert Range. Samples taken at 25 cm stratigraphic spacing. Note the higher and lower frequency cycles in the data series. Lithostratigraphic column is based on field observations and Stewart and Barnes (1966). **(bottom)** MTM spectrum of the magnetic susceptibility data series calculated by Acycle (Li et al., 2019). Black line is robust red noise model (Mann and Lees, 1996) with 90% (thin red line), 95% (dashed red line), and 99% (dashed blue line) confidence intervals. Significant spectral peaks are outlined in boxes consistent with (Berger et al., 1992) theoretical peaks for short eccentricity (125/95 ka), obliquity (29 ka) and precession (18.7/16 ka) at 500 Ma.

 $348.4^{\circ}$ E,  $A_{95} = 8.6^{\circ}$ , N = 60 and is reversed polarity. It agrees with the "shallow" paleomagnetic poles for the Ediacaran of North America (mean of Laurentia Ediacaran "shallow component" poles,  $6^{\circ}$ S,  $341^{\circ}$ E,  $A_{95} = 19.2^{\circ}$ ; Abrajevitch and Van der Voo, 2010). The "shallow component" is interpreted by (Bono et al., 2014) to be the primary magnetization of the Sept-Île intrusive rocks. A plot of the VGP paleolatitude (great circle distance from the paleopole- $90^{\circ}$ ) (**Figure 4**) as a function of stratigraphic position can be used to determine the magnetostratigraphy of the Rainstorm Member at the Desert Range locality. Multiple samples were collected at each horizon (nominally three samples) to check the robustness of the polarity interpretation for each horizon. VGP latitudes between  $90^{\circ}$  and  $45^{\circ}$  are interpreted to be normal polarity, latitudes between  $-45^{\circ}$  and  $-90^{\circ}$  are interpreted to be reversed polarity. A  $45^{\circ}$  cutoff for polarity determination is

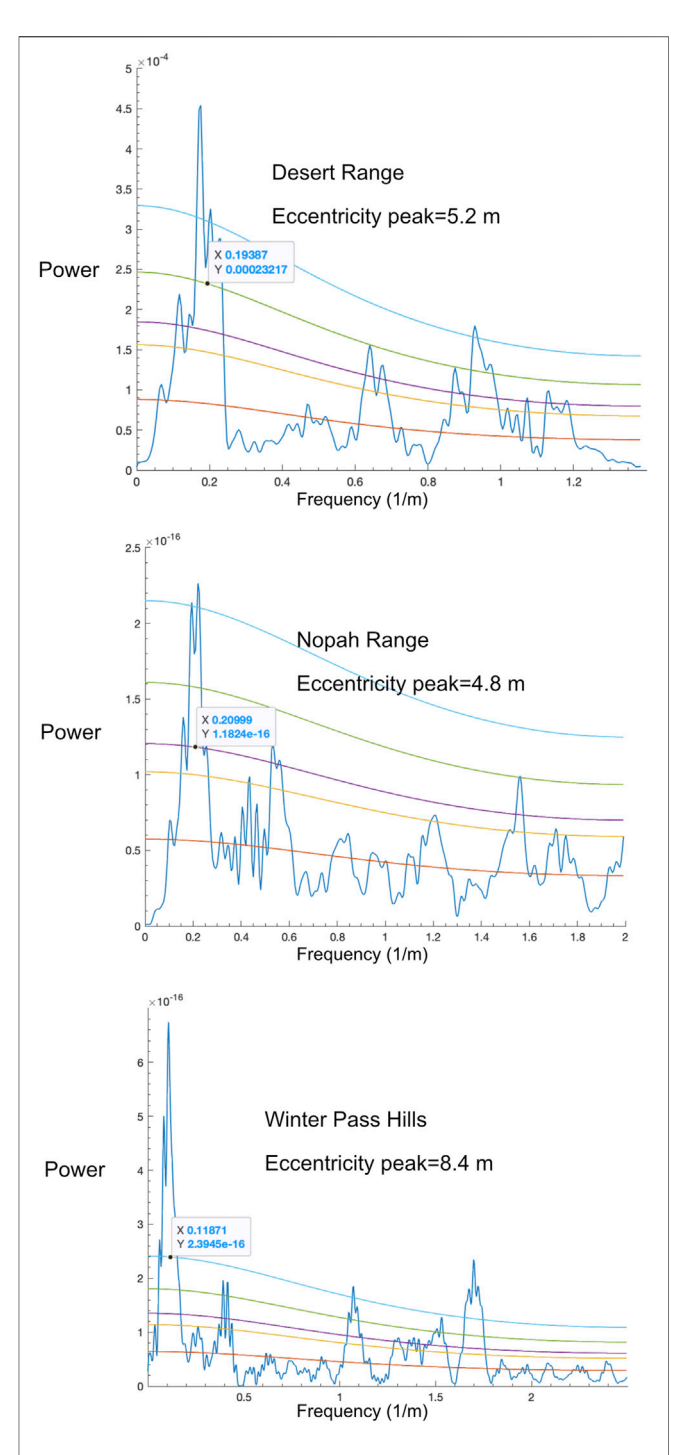


**FIGURE 6 |** MTM power spectra calculated by Acycle from the Desert Range, the Nopah Range, and Winters Pass Hills. The Nopah Range and Winters Pass Hills data are from Minguez et al. (2015). The stratigraphic periods of the highly significant spectral peak assigned to short eccentricity are labeled for each plot. The Desert Range and the Nopah Range both have short eccentricity peaks close to a 5 m period, while the Winters Pass Hills has a short eccentricity peak with a longer stratigraphic period indicating a higher SAR. These relationships in SAR will be used to produce a combined stratigraphy from these three localities of the Rainstorm Member.

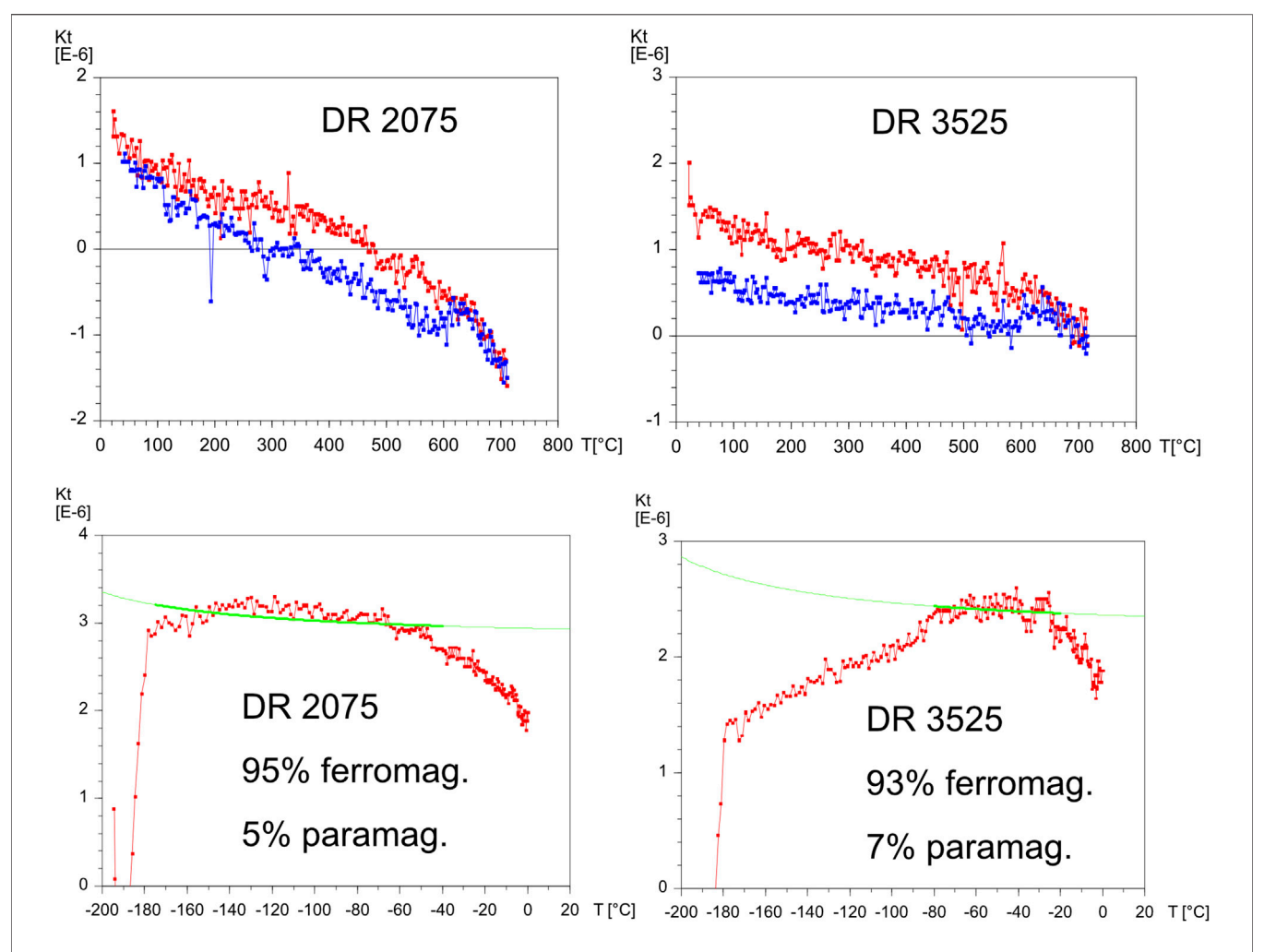


FIGURE 7 | Magneti susceptibility vs temperature plots for Rainstorm Member samples. The top plots show the magnetic susceptibility behavior between room temperature (nominally 20°C) and 700°C. Red data is the heating curve, blue is the cooling curve. Note magnetic susceptibility shows evidence of a decrease during heating at about 680°C suggesting hematite as the main magnetic mineral carrying the susceptibility. The cooling curves both show a decrease at about 580°C, suggesting magnetite may have been destroyed during the heating. The bottom two plots show the magnetic susceptibility behavior between liquid nitrogen temperatures (–196°C) and 0°C. The poor fit of the 1/T paramagnetic hyperbola (green) to the data suggests that most of the susceptibility is carried by ferromagnetic, rather than paramagnetic, minerals. The data shown in the top plots would suggest that ferromagnetic mineral is hematite.

based on (Deenen et al., 's 2011) analysis of paleosecular variation. If at least one sample in a horizon falls within these bounds a polarity interpretation is made. If none of the samples in a horizon can be assigned a polarity under these conditions, the horizon's polarity is designated indeterminate. At the bottom of the section, the Johnnie Oolite's polarity is indeterminate. From 1 to 7 m the section is normal polarity. From 7 m to 16.5 m in the section is the 9.5 m stratigraphic gap in outcrop. From 18 m to 26 m the section is reversed polarity, followed by a normal polarity interval from 28 m to 30 m. The section is reversed polarity from 33 m to 42 m and returns to normal polarity at the top of the 45 m section. The magnetostratigraphy is fairly straightforward, but has a large 9.5 m gap and a nominal 2 m spacing between horizons with one completely indeterminate horizon directly above the 9.5 m stratigraphic gap.

# **Rock Magnetic Cyclostratigraphy**

The mass normalized magnetic susceptibility ( $\chi$ )data series measured for the unoriented samples has values typically of 4 ×  $10^{-8}$  m³/kg but high values can reach  $1.5 \times 10^{-7}$  m³/kg. (**Figure 5**). The data series shows both high frequency sub-meter/meter scale variability and lower frequency several meter scale variability. Multitaper method (MTM) analysis of the time series using Acycle (Li et al., 2019) with robust red noise modeling (Mann and Lees, 1996) to identify significant spectral peaks is used to calculate the power spectrum. Spectral peaks that rise above the 95% confidence level of the robust red noise (dashed red line in **Figure 5**) are observed at 0.2 cycles/meter (5 m stratigraphic period), 0.65 cycles/m (1.5 m stratigraphic period) and multiple peaks between 0.9 and 1.15 cycles/m (1.1–0.9 m stratigraphic periods). These peaks can be matched quite easily to the Milankovitch peaks for short eccentricity (125–95 ka), obliquity (~29 ka) and precession (18.7)

TABLE 1 | Ferromagnetic vs paramagnetic magnetic susceptibility components.

Sample	Ferromagnetic %	Paramagnetic %
DR0000	76.9	23.1
DR0100	90.6	9.4
DR0600	92.1	7.9
DR2075	95.2	4.8
DR2550	57.7	42.3
DR3525	92.8	7.2

and 16 ka) calculated for 500 Ma by Berger et al. (1992). Using COCO (Correlation Coefficient) analysis from Acycle, a significant fit of these spectral peaks to the Berger et al. (1992) theoretical cycles yields a sediment accumulation rate (SAR) for the Rainstorm member of 5.3 cm/ka indicating that the 45 m of section was deposited in 849 ka.  $\chi$  data series from Minguez et al. (2015) indicates strong, significant short eccentricity peaks at 4.8 m stratigraphic period for the Nopah Range and 8.4 m stratigraphic period for the Winters Pass Hills (**Figure 6**). The Desert Range Rainstorm Member eccentricity peak by comparison is 5.2 m when the center of the peak is chosen. These results show that the SARs are nearly the same for the Nopah Range and Desert Range localities of the Rainstorm Member and approximately 1.67 times faster for the Winters Pass Hills locality. We will use these results to combine the magnetostratigraphic and isotopic data from all three localities.

# **Rock Magnetic Analysis**

In order to identify the magnetic minerals in the Rainstorm Member and determine the magnetic minerals carrying the predominance of the magnetic susceptibility, magnetic susceptibility versus temperature experiments were conducted on a subset of Rainstorm Member cyclostratigraphy samples. In the high temperature experiments, samples heated from room temperature up to 700°C, show the signature of a magnetic mineral that loses its magnetism at about 680°C, which is most likely hematite (Figure 7). This observation is in agreement with the red color of the rocks in the Desert Range. However, the magnetic mineralogy of the Rainstorm Member can vary, as well as its color. In Winters Pass Hills the main ferromagnetic mineral is hematite, but at the Nopah Range the ChRMs are carried mainly by magnetite (Minguez et al., 2015). On cooling from 700°C a small decrease compared to the heating curve just below 580°C suggests that magnetite may have been destroyed by the heating. In the low temperature experiments, in which samples warmed from liquid nitrogen temperatures up to 0°C, when the magnetic susceptibility curve is fit with a 1/T hyperbola (Hrouda, 1994; Hrouda et al., 1997), it is clear that almost all the susceptibility is carried by the ferromagnetic minerals in the rock, i.e., hematite, rather than the paramagnetic clay minerals (Figure 7). Of the six samples measured the lowest ferromagnetic component was ~58%, but most were above 90% ferromagnetic (Table 1).

# Carbon Isotope Analysis

The carbon isotope measurements of the carbonate in the Desert Range Rainstorm Member show a steep decrease in  $\delta^{13}$ C from -7 to -10.8 in the bottom 7 m of the section (**Figure 8**). These values and the steep decrease are consistent with the onset of the Shuram carbon isotope excursion observed globally (LeGuerroue, et al.,

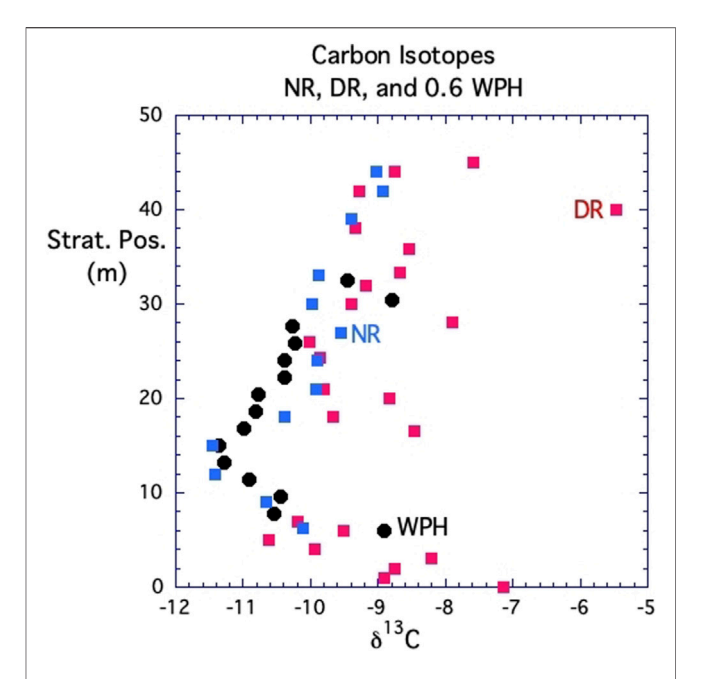


**FIGURE 8** | Carbon isotope stratigraphy for the Desert Range (DR, red squares), Nopah Range (NR, blue squares), and Winters Pass Hills (WPH, black circles) Rainstorm Member samples based on a combined stratigraphy based on the Desert Range and Nopah Range localities have the same SAR of about 5 cm/ka and the Winters Pass Hills has a faster SAR of 8.4 cm/ka. To combine the stratigraphies the WPH stratigraphic positions are multiplied by 0.6. Note that the Shuram carbon isotope excursion is recorded at each locality and that the nadir of the excursion occurs at about 12–14 m in the combined stratigraphy.

2006; Minguez and Kodama, 2017; Gong et al., 2017). The stratigraphic gap in our section between 7 m and 16.5 m is apparently where the nadir of the Shuram excursion occurs in the Desert Range section. Values as low as  $-11.5\,\delta^{13}C$  are typically observed in the section. By 16.5 m in the section the carbon isotope values have recovered to values of about -9.8, but there is a fair amount of scatter in the data from 16.5 m up to the top of the section at 45 m. Despite the scatter there is steady increase in values to about  $-8^\circ$ at the top of the section.

# **DISCUSSION**

The paleomagnetic and the rock magnetic results indicate that hematite carries the ChRM and the magnetic susceptibility  $(\chi)$ . The  $\chi$  cyclostratigraphy results indicate that the hematite records global climate cycles. The paleomagnetic pole calculated from the ChRMs agrees with the "shallow" Ediacaran directions that (Bono et al., 2014) show is the primary Ediacaran direction. These observations and the record of a magnetostratigraphy in the Rainstorm Member supports a primary magnetization for the Rainstorm Member. Specifically, the ChRMs are isolated between 580°C and 680°C, the magnetic susceptibility versus temperature experiments show that the magnetic susceptibility persists until 680°C and that most of the susceptibility is carried by ferromagnetic minerals. The spectral analysis of the magnetic susceptibility data

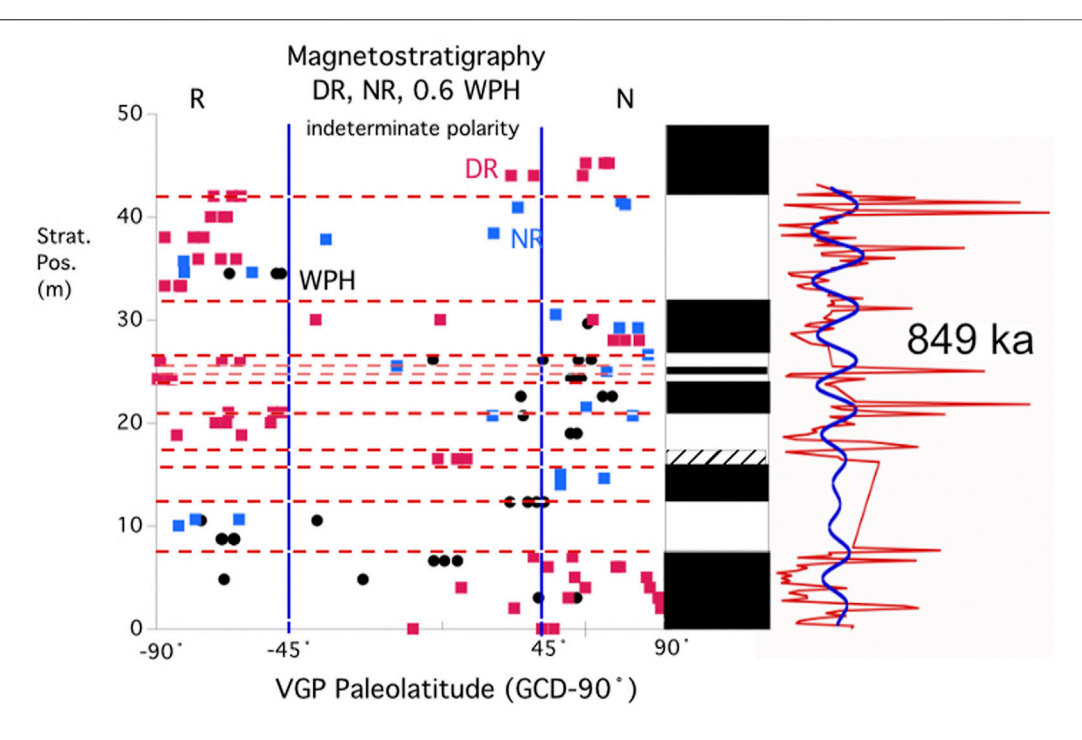


FIGURE 9 | Combined magnetostratigraphy from the Desert Range, Nopah Range and Winters Pass Hills localities. Same color scheme for the data points from the localities as in Figure 8. VGP paleolatitude (GCD-90") is plotted as a function of stratigraphic position combined in the same manner is in Figure 8 (carbon isotope plot). The rules for determining the polarity of each horizon are given in the text. Note the nearly meter stratigraphic spacing for the combined stratigraphy yielding a high resolution magnetostratigraphy that records 11 polarity intervals in the 45 m section. The magnetic susceptibility data series for the Desert Range is shown on the right (in red), with the data filtered (Gaussian filter, calculated by Acycle) at short eccentricity plotted on top (in blue). Assuming an SAR of 5.3 cm/ka from the Desert Range cyclostratigraphy, the duration of the 45 m section is 849 ka. This yields a reversal rate of 13 R/Ma.

series shows significant spectral peaks that can be matched to short eccentricity, obliquity, and precession Milankovitch cycles in the Ediacaran. Correlation coefficient analysis (COCO) indicates a sediment accumulation rate (SAR) of 5.3 cm/ka for the Rainstorm Member in the Desert Range. These results strongly support an early origin, likely depositional, for the ferromagnetic mineral, hematite, carrying the magnetic susceptibility.

The cyclostratigraphy at the Desert Range, the Nopah Range, and Winters Pass Hills localities can be used to construct a combined magnetostratigraphy from these three exposures of the Rainstorm Member. The short eccentricity (95-125 ka) peaks at the Nopah Range and the Desert Range both have a stratigraphic thickness period of ~5 m, and hence these sections have similar SARs (~5m/100 ka). Therefore, their independent magnetic polarity stratigraphies can be combined without any adjustments to the stratigraphic positions of their sampling horizons. The Winters Pass Hills locality has a short eccentricity peak with an 8.4 m stratigraphic thickness period indicating a faster SAR (~8.4m/100 ka). Therefore, the stratigraphic positions of horizons in the Winters Pass Hills section should be multiplied by 5/8.4 = 0.6 to place its sampling horizons in an equivalent time scale before its magnetic polarity stratigraphy can be combined with the Desert Range and the Nopah Range magnetostratigraphies. The carbon isotope results from all three localities can be combined in this manner

to check this approach for combining the three locality sections stratigraphically using the cyclostratigraphy. The combined carbon-isotope stratigraphy shows a good match of carbon-isotope values between the three sections (**Figure 8**). Also, it is apparent that the 9.5 m stratigraphic gap in the Desert Range section is filled by data from the Nopah Range and Winters Pass Hills.

When the magnetic polarity stratigraphy from the three Rainstorm Member localities are combined in this manner, using the cyclostratigraphy, a high-resolution magnetostratigraphy results (Figure 9). The sampling interval is decreased to slightly more than 1 m. Thirty-eight horizons are spaced over 45 m of section, with an average spacing of 1.2 m. Using the SAR of 5.3 cm/ka indicates that this stratigraphic spacing is a temporal spacing of about 23 ka. The same rules used to determine the magnetostratigraphy for the Desert Range section (Figure 4) can be applied to the combined magnetostratigraphy. In the resulting combined magnetostratigraphy, there are some horizons in which all the samples are indeterminate. These horizons typically occur at polarity interval boundaries. They could have resulted from unresolved magnetization overprinting, or they may have deposited during polarity transitions. In some instances, samples with opposite polarities occur at nearly the same stratigraphic level, but this behavior occurs at polarity interval boundaries. It can be attributed to the stratigraphic position inaccuracies of combining the stratigraphic sections.

The resulting combined magnetostratigraphy is based on the Desert Range locality with an SAR of 5.3 cm/ka determined by COCO from the cyclostratigraphy. This rate can be used to estimate the duration of the 45 m section. The section was deposited over 849 ka. Therefore, 11 polarity intervals observed with the high-resolution, combined magnetostratigraphy in 849 ka indicates a reversal frequency of 13 R/Ma. This is slightly higher than the highest frequency observed in the past 170 Ma of 10–12 R/Ma which occurred during the seafloor magnetic anomaly-calibrated Jurassic/early Cretaceous time period.

Rooney et al.'s age estimate for the Shuram carbon isotope excursion between 574 Ma and 567 Ma suggests that the Rainstorm member, which records the early stages of the Shuram excursion is about 574 Ma in age. This age estimate makes the reversal frequency of 13 R/Ma about 27 Ma older than the cyclostratigraphy-calibrated reversal frequency of 20 R/Ma that Levashova et al. (2021) estimated for the Zigan Formation. It shows that reversal frequencies were high, but also highly variable during the Ediacaran. It is interesting to note that our reversal frequency estimate is close in age to the 565 Ma very low field intensity reported by Bono et al. (2019) for the Sept-Île intrusive rocks.

# CONCLUSION

Rock magnetic cyclostratigraphy and paleomagnetic polarity stratigraphy at three localities in the southwestern United States of the Rainstorm Member of the Ediacaran Johnnie Formation produced a high-resolution, combined magnetostratigraphy for the age of the Shuram carbon isotope excursion at 574 Ma. This reversal stratigraphy is precisely time-calibrated by rock magnetic cyclostratigraphy and yields a reversal frequency of 13 R/Ma for the time period just before the very low field intensity observed in the Sept-Île intrusive rocks at 565 Ma (Bono et al., 2019). Given the recent cyclostratigraphy-calibrated reversal frequency of 20 R/Ma from the Zigan Formation (Levashova et al., 2021) at 547 Ma, our results show that reversal frequency was high but fluctuated during the Ediacaran.

#### REFERENCES

- Abrajevitch, A., and Van der Voo, R. (2010). Incompatible Ediacaran Paleomagnetic Directions Suggest an Equatorial Geomagnetic Dipole Hypothesis. *Earth Planet. Sci. Lett.* 293, 164–170. doi:10.1016/j.epsl.2010.02.038
- An, Z., Jiang, G., Tong, J., Tian, L., Ye, Q., Song, H., et al. (2015). Stratigraphic Position of the Ediacaran Miaohe Biota and its Constrains on the Age of the Upper Doushantuo  $\delta$  13 C Anomaly in the Yangtze Gorges Area, South China. *Precambrian Res.* 271, 243–253. doi:10.1016/j.precamres.2015.10.007
- Bazhenov, M. L., Levashova, N. M., Meert, J. G., Golovanova, I. V., Danukalov, K. N., and Fedorova, N. M. (2016). Late Ediacaran Magnetostratigraphy of Baltica: Evidence for Magnetic Field Hyperactivity? Earth Planet. Sci. Lett. 435, 124–135. doi:10.1016/jepsl.2015.12.01510.1016/j.epsl.2015.12.015
- Berger, A., Loutre, M. F., and Laskar, J. (1992). Stability of the Astronomical Frequencies over the Earth's History for Paleoclimate Studies. Science 255, 560–566. doi:10.1126/science.255.5044.560

## **DATA AVAILABILITY STATEMENT**

The datasets presented in this study can be found in online repositories. The names of the repository/repositories and accession number(s) can be found below: doi.org/10.7288/V4/MAGIC/19237.

# **AUTHOR CONTRIBUTIONS**

KK planned the study, organized and participated in the collection of the samples, measured the paleomagnetic samples, analyzed the data and wrote the paper.

# **FUNDING**

This work was funded in part of United States National Science Foundation grant EAR-1322002 to the author.

## **ACKNOWLEDGMENTS**

The students of Lehigh University EES 405 graduate paleomagnetism class, Adam Benfield, Joshua Gonzales, and Frank Tetto conducted the paleomagnetic sampling of the Desert Range Rainstorm Member in May 2018. Dr. Spencer Lodge of the Desert National Wildlife Refuge provided important guidance to and within the sampling locality. He also served as a liaison to Nellis Air Force Base during the sampling field trip and to the local Native American Tribal Council. Joshua Gonzales conducted the rock magnetic cyclostratigraphy study reported here. We thank both the Nellis Air Force Base and the Desert National Wildlife Refuge for their permission to sample the Desert Range locality. We particularly thank Amy Sprunger, Director of the Desert National Wildlife Refuge for her invaluable help with the logistics and obtaining permission from the local tribal council for this sampling trip. The cyclostratigraphy and paleomagnetic data are available in the MagIC database at https://earthref.org/MagIC/16661/d682ee3cb129-4f61-bd79-18303b9482b6.

- Bono, R. K., and Tarduno, J. A. (2014). A Stable Ediacaran Earth Recorded by Single Silicate Crystals of the Ca. 565 Ma Sept-Iles Intrusion. Geology 43, 131–134. doi:10.1130/Ge6247.1
- Bono, R. K., Tarduno, J. A., Nimmo, F., and Cottrell, R. D. (2019). Young Inner Core Inferred from Ediacaran Ultra-low Geomagnetic Field Intensity. *Nat. Geosci.* 12, 143–147. doi:10.1038/s41561-018-0288-0
- Cocks, L. R. M., and Torsvik, T. H. (2011). The Palaeozoic Geography of Laurentia and Western Laurussia: A Stable Craton with mobile Margins. *Earth-Science Rev.* 106, 1–51. doi:10.1016/j.earscirev.2011.01.007
- Condon, D., Zhu, M., Bowring, S., Wang, W., Yang, A., and Jin, Y. (2005). U-pb Ages from the Neoproterozoic Doushantuo Formation, China. *Science* 308, 95–98. doi:10.1126/science.1107765
- Deene, M. H. L., Langereis, C. G., van Hinsbergen, D. J. J., and Biggin, A. J. (2011). Geomagnetic Secular Variation and the Statistics of Palaeomagnetic Directions. *Geophys. J. Int.* 186, 509–520. doi:10.1111/j.1365-246x.2011.05050.x
- Gallet, Y., Pavlov, V., and Korovnikov, I. (2019). Extreme Geomagnetic Reversal Frequency during the Middle Cambrian as Revealed by the Magnetostratigraphy of the Khorbusuonka Section (Northeastern

- Siberia). Earth Planet. Sci. Lett. 528, 115823. doi:10.1016/j.epsl.2019.115823
- Gong, Z., Kodama, K. P., and Li, Y. X. (2019). Paleomagnetism and Rock Magnetic Cyclostratigraphy of the Ediacaran Doushantuo Formation, South China: Constraints on the Remagnetization Mechanism and the Encoding Process of Milankovitch Cycles. *Palaeogeogr. Palaeoclimatol. Palaeoecol.* 528, 232–246. doi:10.1016/j.palaeo.2019.05.002
- Gong, Z., Kodama, K. P., and Li, Y. X. (2017). Rock Magnetic Cyclostratigraphy of the Doushantuo Formation, South China and its Implications for the Duration of the Shuram Carbon Isotope Excursion. *Precambrian Res.* 289, 62–74. doi:10.1016/j.precamres.2017.12.002
- Hrouda, F., Jelinek, V., and Zapletal, K. (1997). Refinement of the Technique for Susceptibility Resolution into Ferromagnetic and Paramagnetic Components. *Geophys. J. Int.* 129, 715–719. doi:10.1111/j.1365-246X.1997.tb04506.x
- Hrouda, Frantisek. (1994). A Technique for the Measurement of thermal Changes of Magnetic Susceptibility of Weakly Magnetic Rocks by the CS-2 Apparatus and KLY-2 Kappabridge. *Geophys. J. Int.* 118, 604–612. doi:10.1111/j.1365-246X.1994.tb03987.x
- Hüsing, S. K., Beniest, A., van der Boon, A., Abels, H. A., Deenen, M. H. L., Ruhl, M., et al. (2014). Astronomically-calibrated Magnetostratigraphy of the Lower Jurassic marine Successions at St. Audrie's Bay and East Quantoxhead (Hettangian-Sinemurian, Somerset, UK). Palaeogeog., Palaeoclimat., Palaeoecol. 403, 43–56. doi:10.1016/j.palaeo.2014.03.022
- Kent, D. V., Olsen, P. E., and Muttoni, G. (2017). Astrochronostratigraphic Polarity Time Scale (APTS) for the Late Triassic and Early Jurassic from continental Sediments and Correlation with Standard marine Stages. *Earth-Science Rev.* 166, 153–180. doi:10.106/j.earscirev.2016.12.01410.1016/j.earscirev.2016.12.014
- Kirschvink, J. L. (1980). The Least-Square Line and Plane and the Analysis of Paleomagnetic Data. *Geophys. J. R. Astronomical Soc.* 62, 699–718.doi:10.1111/ j.1365-246X.1980.tb02601.x
- Knoll, A. H., and Carroll, S. B. (1999). Early Animal Evolution; Emerging Views from Comparative Biology and Geology. Science 284 (5423), 2129–2137. doi:10.1126/science.284.5423.2129
- Kodama, K. P., and Hinnov, L. A. (2015). Rock Magnetic Cyclostratigraphy. Oxford: Wiley-Blackwell, 165.
- Le Guerroué, E., Allen, P. A., Cozzi, A., Etienne, J. L., and Fanning, M. (2006). 50 Myr Recovery from the Largest negativeδ13C Excursion in the Ediacaran Ocean. *Terra Nova* 18, 147–153. doi:10.1111/j.1365-3121.2006.00674.x
- Levashova, N. M., Golovanova, I. V., Rudko, D. V., Danukalov, K. N., Rudko, S. V., Yu, S. R., et al. (2021). Late Ediacaran Magnetic Field Hyperactivity: Quantifying the Reversal Frequency in the Zigan Formation, Southern Urals, Russia. Gondwana Res. 94, 133-142. doi:10.1016/j.gr.2021.02.018
- Li, M., Hinnov, L., and Kump, L. (2019). Acycle: Time-Series Analysis Software for Paleoclimate Research and Education. Comput. Geosciences 127, 12–22. doi:10.1016/j.cageo.2019.02.011
- Li, M., Zhang, Y., Huang, C., Ogg, J., Hinnov, L. A., Wang, H., et al. (2017). Astronomical Tuning and Magnetostratigraphy of the Upper Triassic Xujiahe Formation of South China and Newark Supergroup of North America: Implications for the Late Triassic Time Scale. *Earth. Planet. Sci. Letters* 475, 207–223. doi:10.1016/j.epsl.2017.07.015
- Mann, M. E., and Lees, J. M. (1996). Robust Estimation of Background Noise and Signal Detection in Climatic Time Series. Climatic Change 33, 409–445. doi:10.1007/bf00142586
- Meert, J. G., Levashova, N. M., Bazhenov, M. L., and Landing, E. (2016). Rapid Changes of Magnetic Field Polarity in the Late Ediacaran: Linking the

- Cambrian Evolutionary Radiation and Increased UV-B Radiation. Gondwana Res. 34, 149–157. doi:10.1016/j.gr.2016.01.001
- Minguez, D., Kodama, K. P., and Hillhouse, J. W. (2015). Paleomagnetic and Cyclostratigraphic Constraints on the Synchroneity and Duration of the Shuram Carbon Isotope Excursion, Johnnie Formation, Death Valley Region, CA. Precambrian Res. 266, 395–408. doi:10.1016/j/ precamres.2015.05.03310.1016/j.precamres.2015.05.033
- Minguez, D., and Kodama, K. P. (2017). Rock Magnetic Chronostratigraphy of the Shuram Carbon Isotope Excursion: Wonoka Formation, Australia. *Geology* 45, 567–570. doi:10.1130/G38572.1
- Pavlov, V., and Gallet, Y. (2001). Middle Cambrian High Magnetic Reversal Frequency (Kulumbe River Section, Northwestern Siberia) and Reversal Behaviour during the Early Palaeozoic. Earth Planet. Sci. Lett. 185, 173–183. doi:10.1016/s0012-821x(00)00364-2
- Pavlov, V., and Gallet, Y. (2010). Variations in Geomagnetic Reversal Frequency during the Earth's Middle Age. Geochemisty, Geophys. Geosystems 11, 1–28. doi:10.1029/2009gc002583
- Rooney, A. D., Cantine, M. D., Bergmann, K. D., Gómez-Pérez, I., Al Baloushi, B., Boag, T. H., et al. (2020). Calibrating the Coevolution of Ediacaran Life and Environment. Proc. Natl. Acad. Sci. USA 117, 16824–16830. doi:10.1073/pnas.2002918117
- Stewart, J. H., and Barnes, H. (1966). Precambrian and Lower Cambrian Formations in the Desert Range, Clark County, Nevada. U.S. Geol. Surv. Bull. 1244-A, Changes Stratigraphic Nomencl. by U.S 1965, A38. doi:10.3133/b1244a
- Stewart, J. H. (1970). Upper Cambrian and Lower Cambrian Strata in the Southern Great Basin California and Nevada. U.S. Geol. Surv. Prof. Paper 620, 206 pp. doi:10.3133/pp620
- Tauxe, L., Shaar, R., Jonestrask, L., Swanson-Hysell, N. L., Minnett, R., Koppers,
  A. A. P., et al. (2016). PmagPy: Software Package for Paleomagnetic Data
  Analysis and a Bridge to the Magnetics Information Consortium (MagIC)
  Database. Geochem. Geophys. Geosyst. 17, 2450-2463. doi:10.1002/ 2016gc006307
- Thomson, D. J. (1982). Spectrum Estimation and Harmonic Analysis. *Proc. IEEE* 70, 1055–1096. doi:10.1109/proc.1982.12433
- Van Alstine, D. R., and Gillett, S. L. (1979). Paleomagnetism of Upper Precambrian Sedimentary Rocks from the Desert Range, Nevada. J. Geophys. Res. 84, 4490–4500. doi:10.1029/jb084ib09p04490
- Zijderveld, J. D. A. (1967). "AC Demagnetization of Rocks: Analysis of Results," in *Methods in Paleomagnetism*. Editors D.W. Collinson, K.M. Creer, and S.K. Runcorn (Amsterdam: Elsevier), 254–286.

**Conflict of Interest:** The author declares that the research was conducted in the absence of any commercial or financial relationships that could be construed as a potential conflict of interest.

**Publisher's Note:** All claims expressed in this article are solely those of the authors and do not necessarily represent those of their affiliated organizations, or those of the publisher, the editors and the reviewers. Any product that may be evaluated in this article, or claim that may be made by its manufacturer, is not guaranteed or endorsed by the publisher.

Copyright © 2021 Kodama. This is an open-access article distributed under the terms of the Creative Commons Attribution License (CC BY). The use, distribution or reproduction in other forums is permitted, provided the original author(s) and the copyright owner(s) are credited and that the original publication in this journal is cited, in accordance with accepted academic practice. No use, distribution or reproduction is permitted which does not comply with these terms.